# Ionization of Excited Atoms by Intense Single-Cycle THz Pulses

Sha Li and R. R. Jones
*Department of Physics, University of Virginia, Charlottesville, Virginia 22904, USA*
(Received 29 July 2013; revised manuscript received 19 January 2014; published 9 April 2014)

We have employed intense, single-cycle THz pulses to explore strong-field ionization of low-lying Na Rydberg states in the low-frequency limit. At the largest fields used, $F \simeq 430$ kV/cm, electrons with energies up to 60 eV are created. The field ionization threshold is greater than expected for adiabatic "over-the-barrier" ionization and is found to scale as $n^{-3}$. In addition, for a given field amplitude, higher energy electrons are produced during the ionization of the most tightly bound states. These observations can be attributed to the suppression of scattering from the nonhydrogenic ion core, the long times required for Rydberg electrons to escape over the barrier in the field-dressed Coulomb potential, and the failure, in the single-cycle limit, of the standard prediction for electron energy transfer in an oscillating field. The latter, in particular, holds important implications for future strong-field experiments involving the interaction of ground-state atoms and molecules with true single-cycle laser fields.

DOI: 10.1103/PhysRevLett.112.143006 PACS numbers: 32.80.Rm, 32.80.Ee

The exaggerated properties of Rydberg atoms, including small binding energies, high state densities, and long time scales, make them excellent systems for exploring atomic ionization dynamics in pulsed and oscillating fields [1]. A variety of field-ionization mechanisms have been identified in the rf [2–8], microwave [2,10,11], and THz [12] spectral regions. Different mechanisms dominate the ionization process in different regimes, delineated by comparing the time and frequency scales in the field to the corresponding natural atomic scales. Measurements of requisite ionization fields versus $n$ identify boundaries between ionization regimes, and play a key role in the discovery of new ionization pathways. In the long-pulse and low-frequency regime, over-the-barrier (OTB) ionization involving little or no energy transfer from the field to the electron occurs with an $n^{-4}$ threshold field scaling [1,3–5]. Conversely, in a short unipolar pulse, ionization occurs by impulsive energy transfer to the electron, requiring a larger field proportional to $n^{-1}$ [7–9]. More complex dynamics are reflected in other $n$ dependencies, e.g., $n^{-5}$ [10] or $n^{-2}$ [12]. Beyond fundamental interest, insights gleaned from Rydberg atom measurements play an important role in understanding strong-field processes involving ground-state atoms or molecules, from tunneling or over-the-barrier ionization [13], to nonadiabatic ladder climbing [14,15], to the development [16–18] and refinement [19] of the simpleman's model of energy transfer to electrons in an oscillating field.

Here we describe experiments in which single-cycle THz fields (see Fig. 1) are used to ionize atoms in low-lying Rydberg states of Na, $6 \leq n \leq 15$. The field period (and duration), $T \simeq 4$ ps, is longer than the Kepler period, $\tau_K = 2\pi n^3$, and the field frequency $\omega \simeq 0.20$ THz is less than the spacing between adjacent $n$ states, $\Delta E_n \simeq 1/n^3$, for all levels studied [20]. Thus, based on these atomic scales, the experiments fall in the low-frequency, long-pulse regime [21]. Surprisingly, we find that the threshold fields are greater than expected for adiabatic ionization, and scale as $n^{-3}$ rather than $n^{-4}$. Classical simulations reproduce the observed scaling, attributing it to both the suppression of nonhydrogenic core scattering and the long times, $> \tau_K$, that electrons require to travel over the saddle point in the field-dressed Coulomb potential.

The electron energy distributions also suggest new physics associated with the single-cycle nature of the ionizing field. We find, counterintuitively, that electrons originating from the most tightly bound Rydberg states leave the atom with the greatest energies. Moreover, in spite of the fact that field-driven, high-energy electron backscattering [23–25] does not occur in the single-cycle field, the electron energies can significantly exceed the simpleman's prediction $\Delta E_{\max} = 2U_p$ for the maximum allowable energy transfer in the absence of rescattering. Here $U_p = F_{\max}^2/4\omega^2$ is the pondermotive energy of a free electron in an oscillating field with peak amplitude $F_{\max}$ and frequency $\omega$. These observations reflect the failure of two standard tenets of strong field energy transfer which, in turn, will have a substantial impact on experiments that require distinguishability of direct and rescattered electrons in intense single-cycle laser fields.

In the experiment, Na atoms in a thermal beam in vacuum are laser excited to $nd$ Rydberg states at the center of a time-of-flight (TOF) spectrometer using two, 5 ns dye laser pulses. The Rydberg atoms are then exposed to an intense single-cycle THz pulse. The $Na^+$ ion or electron yield is measured as a function of the peak THz field. Ions produced in the interaction region are pushed toward a microchannel plate detector by a small $\simeq$50 V/cm field pulse applied to the interaction region. The energy distribution of electrons ejected toward the microchannel plate is determined from their TOF.

 

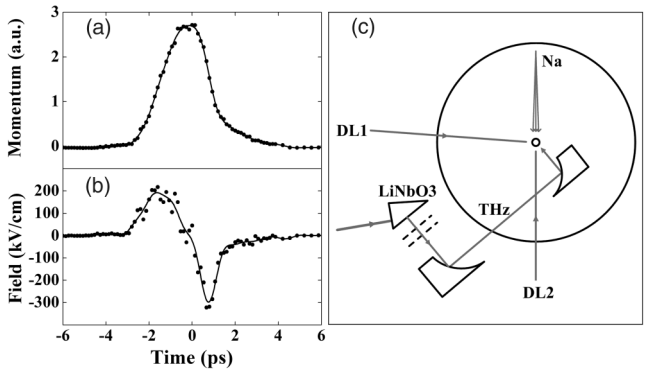


FIG. 1. (a) Maximum momentum transfer from a THz field to low-energy photoelectrons as a function of delay between the electron emission and the temporal center of the THz pulse (points) and FFT filtered data (solid line). (b) Single-cycle THz waveform derived from raw data (points) and smoothed data (solid line) in (a). The variation of the data points about the smooth curve reflects the statistical uncertainty which is ~10% near the extrema. (c) Schematic of the THz ionization experiment. DL1 and DL2 denote dye lasers that drive the $3s - 3p$ and $3p - nd$ transitions, respectively. The dashed lines across the THz beam represent wire-grid polarizers.

The two dye lasers, which are pumped at a 15 Hz repetition rate by the harmonics of a Nd:YAG laser, are collinearly polarized along the spectrometer axis and sequentially excite $3s$ ground-state atoms, through an intermediate $3p_{1/2}$ level, to the $nd$ Rydberg state of interest. The lasers are focused by 50 cm lenses and enter the interaction region at right angles. The THz pulse arrives ~20 ns after the Rydberg excitation.

The intense THz pulses are generated in $LiNbO_3$ via optical rectification of 150 fs, 790 nm, 20 mJ, Ti:sapphire laser pulses. A tilted-pulse-front-pumping scheme enhances the optical to THz conversion efficiency [26,27]. The THz intensity is varied using a variable attenuator composed of two wire-grid polarizers. Two off-axis parabolic mirrors are used to focus the THz beam into the interaction region [Fig. 1(c)]. The dye laser and THz beams cross at ~45 deg angles and have parallel linear polarizations. The ≈2 mm diameter of the focused THz beam is much greater than that of either dye laser. Thus, the THz field is uniform over the Rydberg excitation volume.

Prior to the ionization experiments, we measure the THz waveform in the interaction region using photoelectron "streaking" [28,29]. The second dye laser is replaced by a 150 fs, 395 nm frequency-doubled Ti:sapphire laser pulse, which ionizes atoms in the $3p_{1/2}$ level, creating ~100 meV photoelectrons. The momentum transfer $\Delta p$ from the THz field to the photoelectrons is determined from the electron TOF as a function of the delay $t_0$ between the ionization and THz pulses. The 45 deg crossing angle between the THz and ionization pulses limits the temporal resolution to ~400 fs. As shown in Fig. 1, $\Delta p$ can be substantial, with a maximum energy transfer of 100 eV.

Relative to the THz duration, a photoelectron spends an insignificant amount of time near its parent ion where the Coulomb field is non-negligible. Thus, the integrated influence of the Coulomb field on the continuum electron is negligible compared to the effect of the strong THz pulse [19]. To an excellent approximation, $\Delta p(t_0) = -\int_{t_0}^{\infty} F(t)dt = \alpha[A(\infty) - A(t_0)]$ where $F(t)$ and $A(t)$ are the THz field and vector potential, respectively, and $\alpha$ is the fine-structure constant. Inspection of Fig. 1(a) shows that $\Delta p = 0$ for large negative and large positive delays [30]. Accordingly, without loss of generality, we can define $A(-\infty) = A(\infty) = 0$ such that $\Delta p(t_0) = -\alpha A(t_0)$. This last expression is the essence the simpleman's model [16–18] and can be trivially inverted to give the THz field $F(t) = \frac{d}{dt}(\Delta p)$.

The THz field [Fig. 1(b)], derived from the momentum transfer data in Fig. 1(a), appears as a single-cycle sine waveform with a pronounced frequency chirp and an amplitude asymmetry between the negative and positive half cycles. The positive half cycle has an amplitude (duration) that is ~2/3 (~3/2) that of the negative half cycle. To place the energy transfer in context with other strong-field experiments, we use the average frequency during each half cycle to consistently define, $U_p \sim 16 \pm 2$ eV for both half cycles of the pulse in Fig. 1(b).

Beyond determining the THz field in the interaction region, the streaking measurement enables an examination of energy transfer in the single-cycle limit. Like strong-field ionization of ground state systems, our continuum electrons are "born" near the nucleus with approximately zero kinetic energy. However, unlike a typical ionization experiment, we control the time of ionization within the waveform. We find that two tenets of strong-field energy transfer—(i) in the absence of rescattering the maximum energy acquired by an electron in an oscillating field is $\Delta E_{\max} = 2U_p$, and (ii) an electron ionized at the peak of an oscillating field obtains negligible drift energy—do not apply. Currently, these rules are relied upon to calibrate laser intensities [31–33], distinguish rescattered from directly ionized electrons to enable molecular imaging [31,34,35] or measure the carrier-envelope phase in few-cycle laser pulses [36,37], or to interpret dynamics relevant to a variety of strong-field processes [33,38–41]. However, they fail completely in the single-cycle limit due to the breakdown of the slowly varying envelope approximation.

In a many-cycle pulse, the extrema of the vector potential $|A_{\max}| = F_{\max}/\omega$ occur at the zeros of the electric field, and $A = 0$ at the field extrema. However, for a single-cycle sine wave, $|A_{\max}| = 2F_{\max}/\omega$ at the zero crossing and $|A| = F_{\max}/\omega$ at the field extrema. Accordingly, $\Delta E = 8U_p$ and $2U_p$ for ionization at the central zero crossing and field maxima, respectively. The momentum transfer data in Fig. 1(a) support these predictions, with a maximum energy transfer of $(6.2 \pm 1.2)U_p$ at the zero crossing and $\sim 2U_p$ at the field extrema.

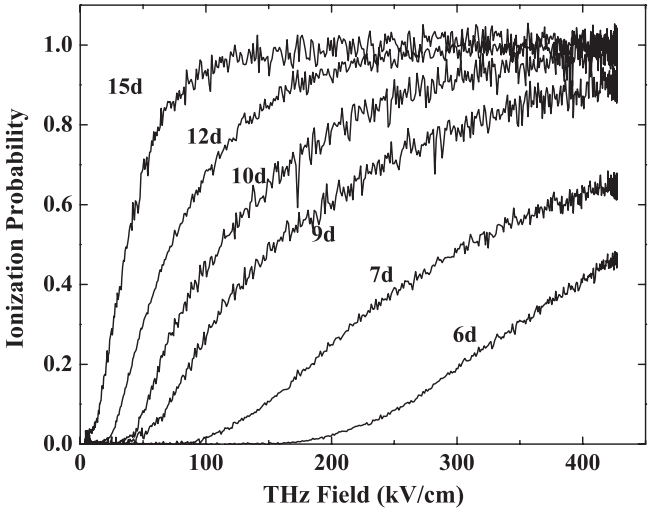


FIG. 2. Measured ionization probability as a function of $F_{\max}$ for several $nd$ states. The THz field is calibrated using THz streaking measurements (Fig. 1).

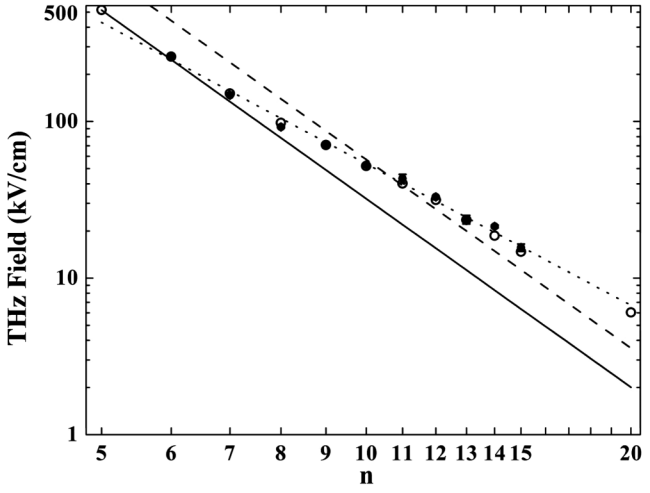


FIG. 3. Peak THz field required for 10% ionization as a function of $n$. (filled circle) Experimental data; (open circle) CTMC calculation; (dotted line) best fit, $n^{-3}/96$, to experimental data; predicted adiabatic ionization thresholds $\mathcal{F}_H = n^{-4}/9$ (dashed line) and $\mathcal{F}_0 = n^{-4}/16$ (solid line) for hydrogenic and nonhydrogenic Rydberg atoms, respectively. The experimental fields have been scaled by 1.05x to obtain the best agreement with the calculation. Experimental error bars are comparable to the size of the data symbols and are not visible for all points.

We have used the single-cycle pulses to measure the ionization yield, as a function of $F_{\max}$, for a range of states with $n \geq 5$. No ionization from the $5d$ level was observed. When the 50 V/cm clearing field is replaced with a 7 kV/cm field-ionization ramp, no population transfer to bound states with $n > 15$ is observed for any initial state or THz field strength, indicating purely adiabatic ionization. For $n \geq 10$, the ionization yield saturates for large THz fields. Assigning unit ionization probability to this saturated signal provides the ionization yield to probability calibration.

Figure 2 shows representative ionization probability versus $F_{\max}$ curves for $6 \leq n \leq 15$. From these data we define $F_{10\%}$ as the peak THz field that produces 10% ionization for a given $n$ state. Measured values of $F_{10\%}$ versus $n$ are plotted in Fig. 3. Notably, the measured thresholds differ significantly from those predicted for adiabatic OTB ionization, exhibiting a novel $n^{-3}$ dependence rather than the expected $n^{-4}$ scaling. The $n^{-3}$ scaling reflects a suppression of adiabatic ionization for $n > 6$ due to the short period and duration of the THz field relative to atomic time scales distinct from $\tau_K$.

Adiabatic OTB ionization is energetically allowed provided $F > E^2/4$, where $E$ is the electron's energy in the field. For ground-state atoms, the electron suffers only a small second-order Stark shift in the field, so $E^2/4 \simeq n^{-4}/16 \equiv \mathcal{F}_0$. In classical terms, OTB ionization can proceed provided the electron has sufficient time to encounter and pass over the barrier while $F > \mathcal{F}_0$. For ground-state atoms this time is $< \tau_K$.

The situation is more complicated for Rydberg states [1]. Upon the application of our THz field, the $nd$ states are projected onto a manifold of Stark states, which have different dipole orientations and accompanying linear Stark shifts. For hydrogenic atoms, the saddle point at threshold is only accessible to the most "downhill" Stark state. When the negative energy shift of this state is taken into account, its OTB ionization threshold $\mathcal{F}_H = n^{-4}/9$ defines the minimum field at which ionization can occur. Due to their orientation, the other Stark states have negligible overlap with the saddle when $F = \mathcal{F}_H$. They require a larger "hole" in the binding potential and, accordingly, a larger field to ionize [42].

In nonhydrogenic atoms like Na, Stark states are coupled by the non-Coulombic potential, and Landau-Zener transitions between states with different orientations can occur as the field rises from zero to its maximum [1,5]. Classically, a bound electron can scatter from one Stark trajectory to another each time the electron passes near the nonhydrogenic ion core. If the scattering rate is sufficiently high compared to the slew rate of the field, the electron can have zero net Stark shift during the rise of the field. Therefore, it can ionize at (or near) $\mathcal{F}_0$, as predicted for atoms with no Stark shift [3].

For the lowest $n$ states studied, the thresholds approach $\mathcal{F}_0 = n^{-4}/16$, indicating nonhydrogenic OTB ionization and a core-scattering rate larger than the slew rate of the THz field. For higher $n$, the core-scattering rate decreases and the ionization thresholds rise above $\mathcal{F}_0$. This is consistent with the transition from non-hydrogen-like to hydrogenlike OTB ionization observed previously for ramped-field ionization [5]. In the presence of this effect alone, we would expect a gradual transition from thresholds scaling as $\mathcal{F}_0$ at low $n$ to $\mathcal{F}_H$ at high $n$. Interestingly, for the highest $n$ states studied, the ionization thresholds significantly exceed $\mathcal{F}_H = n^{-4}/9$. The additional ionization

suppression is caused by the extended time required for higher-$n$ electrons to traverse the saddle point in the field-dressed potential.

For $F_{\max} \simeq \mathcal{F}_0$, the outer turning point of the downhill orbit is located near the saddle point at a radius $R_0 = 4n^2$. Thus, the orbit is nearly twice as large as in zero field. For the states studied, the extra distance the electron must cover, accompanied with its extremely low radial velocity between $r = 2n^2$ and $r = R_0$, leads to a nearly fourfold increase in the orbit period (140 fs and 2.3 ps for $n = 6$ and $n = 15$, respectively). Provided $F_{\max}$ is above threshold, ionization is energetically allowed but can only occur if the electron has sufficient time to traverse the saddle. For $n > 6$ this dynamical criterion can be satisfied by increasing $F_{\max}$, which in turn (i) increases the interval during which ionization is energetically allowed, (ii) increases the radial velocity of electrons traveling towards the saddle, and (iii) moves the saddle point to smaller $r$.

The preceding arguments are fully supported by a classical trajectory Monte Carlo (CTMC) simulation. The calculation (details in Ref. [12]) assumes an asymmetric field like that shown in Fig. 1, and a soft Coulomb potential $V = -1/\sqrt{r^2 + r_0^2}$ to simulate the nonhydrogenic core. Larger $r_0$ values result in a greater rate of scattering between Stark states. The computed threshold for $n = 15$ is found to be independent of physically reasonable values of $r_0$ and agrees with the measured value within 5%. With the field calibration fixed, we adjust $r_0$ to give the best overall agreement between the simulated and experimental thresholds (Fig. 3). The optimum value $r_0 = 0.03$ is not critical and reasonable agreement is obtained for $0.01 \leq r_0 \leq 0.1$. Calculations for $n = 20$ and $n = 5$ confirm the further growth of the suppression at higher $n$ and its disappearance at low $n$, respectively.

Figure 4 shows the electron energy distributions produced during the ionization of several $n$ states for $F_{\max} = 430$ kV/cm. Counter to expectations for multiphoton or OTB ionization in a multicycle field, electrons with the highest energies are produced from states that are more tightly bound. Perturbatively, for a given multiphoton order, higher-energy electrons would be produced from the most weakly bound states. For multicycle OTB ionization, the most tightly bound states ionize near the peak of the waveform where the vector potential is small, resulting in reduced momentum transfer as compared to more weakly bound states, which can ionize closer to the zero crossing of the field.

As discussed previously, the situation is different for single-cycle pulses. An electron ionized at a field maximum in a single-cycle sine wave acquires an energy $\Delta E = 2U_p$. In the same field, an electron in a more weakly bound level will ionize on the rising edge of the first half cycle, and ultimately gain less energy from the field. Accordingly, in units of $U_p$, the maximum energy $\Delta E_{\max}$ transferred to an electron from a given $n$ state should decrease as $F_{\max}$ is raised from near, to well above, $F_{10\%}$.

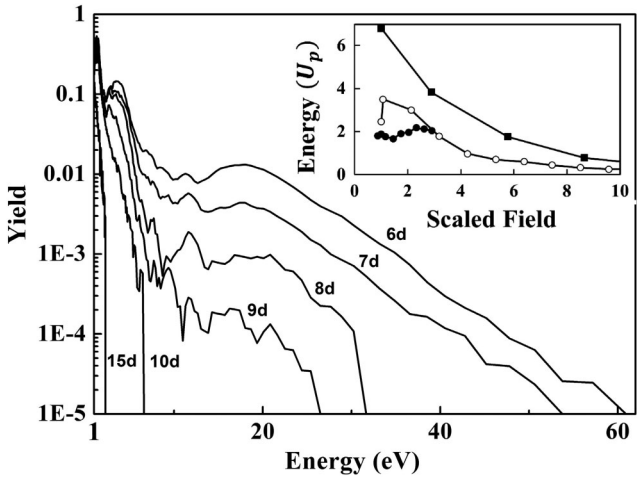


FIG. 4. Electron energy distributions (energy-integrated yields normalized to 1) for different $n$ states ionized by a 430 kV/cm single-cycle THz field. Inset: maximum electron energy as a function of $F_{\max}$ for representative states, $n = 7$ (filled circle), $n = 11$ (open circle), and $n = 15$ (filled square). Error bars are smaller than the data symbols.

The Fig. 4 inset shows $\Delta E_{\max}$ (scaled to $U_p$) as a function of $F_{\max}$ (scaled to $F_{10\%}$) for $n = 7$, 11, and 15. The data shown represent the evolution of analogous results from low to high $n$. For low $n$, with $F_{\max} \simeq F_{10\%}$, ionization occurs near, or slightly after, the peak in the second half cycle such that $\Delta E_{\max} \sim 2U_p$. Since $F_{\max}$ cannot be increased sufficiently to saturate the ionization probability on the rising edge of the pulse, no significant decrease in $\Delta E_{\max}$ is observed for the lowest $n$ states. For intermediate $n$, $\Delta E_{\max} \simeq 2U_p$ for $F_{\max} \simeq F_{10\%}$, as expected for ionization near the peak of the second half cycle in the field. $\Delta E_{\max}$ grows for a modest increase in $F_{\max}$ above $F_{10\%}$, likely due to the greater probability of ionization between the two field maximum, i.e., slightly after (before) the first (second) half cycle. For $F_{\max} \gg F_{10\%}$, $\Delta E_{\max}$ progressively falls as ionization occurs ever earlier on the rising edge of the first half cycle. For high $n$, energies well above $2U_p$ are observed for fields near, to moderately above, threshold. We suspect that this is due to the breakdown of the adiabatic approximation. Electrons ionizing from these states need not reverse direction as they move in their extended orbits over a significant portion of each half cycle of the field. Accordingly, they can acquire non-negligible energy and are effectively "born" before passing over the saddle. This enables them to gain a large kinetic energy from the field, in spite of the fact that they may not actually traverse the saddle until after the peak of the pulse.

In summary, we have explored strong-field ionization of excited atoms using single-cycle THz pulses. We find that adiabatic over-the-barrier ionization is suppressed due to the extended times required for high-$n$ electrons to leave the binding potential, resulting in a novel $n^{-3}$ ionization-field scaling. A similar suppression might influence strong-field

ionization of delocalized electrons from large molecules. We have also shown that, in contrast to ionization in multicycle fields, electrons that are ionized near field extrema acquire substantial energies ($\sim 2U_p$), and those ionized near the zero crossing can obtain much larger energies ($> 6U_p$), even in the absence of rescattering. As experimentally available optical pulses approach the single-cycle limit, the physics underlying our results will impact the interpretation and feasibility of measurements involving ground-state atoms and molecules, particularly those where distinguishing recollision from directly ionized electrons is important, or where mapping electron energy to ionization time is desired.

It is a pleasure to acknowledge helpful conversations with F. Robicheaux and T. Gallagher. This work was supported by the Chemical Sciences, Geosciences and Biosciences Division, Office of Basic Energy Sciences, Office of Science, U.S. Department of Energy.

[1] See T. F. Gallagher, *Rydberg Atoms* (Cambridge University Press, Cambridge, England, 1994), 1st ed., and references therein.
[2] J. E. Bayfield and P. M. Koch, Phys. Rev. Lett. **33**, 258 (1974).
[3] T. W. Ducas, M. G. Littman, R. R. Freeman, and D. Kleppner, Phys. Rev. Lett. **35**, 366 (1975).
[4] T. F. Gallagher, L. M. Humphrey, R. M. Hill, and S. A. Edelstein, Phys. Rev. Lett. **37**, 1465 (1976).
[5] T. H. Jeys, G. W. Foltz, K. A. Smith, E. J. Beiting, F. G. Kellert, F. B. Dunning, and R. F. Stebbings, Phys. Rev. Lett. **44**, 390 (1980).
[6] C. R. Mahon, J. L. Dexter, P. Pillet, and T. F. Gallagher, Phys. Rev. A **44**, 1859 (1991).
[7] C. O. Reinhold, M. Melles, H. Shao, and J. Burdgorfer, J. Phys. B **26**, L659 (1993).
[8] S. Yoshida, C. O. Reinhold, J. Burgdorfer, B. E. Tannian, R. A. Popple, and F. B. Dunning, Phys. Rev. A **58**, 2229 (1998).
[9] C. Wesdorp, F. Robicheaux, and L. D. Noordam, Phys. Rev. Lett. **87** 083001 (2001).
[10] P. Pillet, W. W. Smith, R. Kachru, N. H. Tran, and T. F. Gallagher, Phys. Rev. Lett. **50** 1042 (1983).
[11] M. W. Noel, W. M. Griffith, and T. F. Gallagher, Phys. Rev. Lett. **83**, 1747 (1999).
[12] R. R. Jones, D. You, and P. H. Bucksbaum, Phys. Rev. Lett. **70**, 1236 (1993).
[13] S. Augst, D. Strickland, D. D. Meyerhofer, S. L. Chin, and J. H. Eberly, Phys. Rev. Lett. **63**, 2212 (1989).
[14] M. Lezius, V. Blanchet, D. M. Rayner, D. M. Villeneuve, A. Stolow, and M. Y. Ivanov, Phys. Rev. Lett. **86** 51 (2001).
[15] G. N. Gibson, Phys. Rev. Lett. **89** 263001 (2002).
[16] H. B. van Linden van den Heuvell and H. G. Muller, in *Multiphoton Processes*, edited by S. J. Smith and P. L. Knight (Cambridge University Press, Cambridge, England, 1988).
[17] T. F. Gallagher, Phys. Rev. Lett. **61**, 2304 (1988).
[18] P. B. Corkum, N. H. Burnett, and F. Brunel, Phys. Rev. Lett. **62**, 1259 (1989).
[19] E. S. Shuman, R. R. Jones, and T. F. Gallagher, Phys. Rev. Lett. **101**, 263001 (2008).
[20] Unless otherwise noted, atomic units are used throughout.
[21] The Keldysh parameter $\gamma = \sqrt{(IP/2U_p)}$ is used to delineate the adiabatic and nonadiabatic strong-field ionization boundary for ground-state atoms and molecules. It takes on values $0.1 \leq \gamma \leq 0.66$, suggesting adiabatic ionization at the fields required to ionize the $n$ states studied. However, $\gamma$ derives from a zero-range potential model and alone is not useful for classifying ionization from extended orbitals [22].
[22] T. Topcu and F. Robicheaux, Phys. Rev. A **86**, 053407 (2012).
[23] P. B. Corkum, Phys. Rev. Lett. **71**, 1994 (1993).
[24] B. Walker, B. Sheehy, L. F. DiMauro, P. Agostini, K. J. Schafer, and K. C. Kulander, Phys. Rev. Lett. **73**, 1227 (1994).
[25] G. G. Paulus, W. Nicklich, Huale Xu, P. Lambropoulos, and H. Walther, Phys. Rev. Lett. **72**, 2851 (1994).
[26] J. Hebling, K.-L. Yeh, M. C. Hoffmann, B. Bartal, and K. A. Nelson, J. Opt. Soc. Am. B **25**, B6 (2008).
[27] H. Hirori, A. Doi, F. Blanchard, and K. Tanaka, Appl. Phys. Lett. **98**, 091106 (2011).
[28] R. Kienberger, M. Hentschel, M. Uiberacker, Ch. Spielmann, M. Kitzler, A. Scrinzi, M. Wieland, Th. Westerwalbesloh, U. Kleineberg, U. Heinzmann, M. Drescher, and F. Krausz, Science **297** 1144 (2002).
[29] U. Fruhling, M. Wieland, M. Gensch, T. Gebert, B. Schatte, M. Krikunova, R. Kalms, F. Budzyn, O. Grimm, J. Rossbach, E. Planjes, and M. Drescher, Nat. Photonics **3**, 523 (2009).
[30] This is expected, as the far-field propagating THz pulse has zero area.
[31] C. I. Blaga, J. Xu, A. D. DiChiara, E. Sistrunk, K. Zhang, P. Agostini, T. A. Miller, L. F. DiMauro, and C. D. Lin, Nature (London) **483**, 194 (2012).
[32] Y. Huismans *et al.*., Phys. Rev. Lett. **109**, 013002 (2012).
[33] B. Bergues *et al.*, Nat. Commun. **3**, 813 (2012).
[34] M. Spanner, O. Smirnova, P. B. Corkum, and M. Y. Ivanov, J. Phys. B **37**, L243 (2004).
[35] X.-B. Bian and A. D. Bandrauk, Phys. Rev. Lett. **108** 263003 (2012).
[36] T. Wittman, B. Horvath, W. Helml, M. G. Schatzel, X. Gu, A. L. Cavalieri, G. G. Paulus, and R. Kienberger, Nat. Phys. **5**, 357 (2009).
[37] D. Ray, Z. Chen, S. De, W. Cao, I. V. Litvinyuk, A. T. Le, C. D. Lin, M. F. Kling, and C. L. Cocke, Phys. Rev. A **83**, 013410 (2011).
[38] Th. Weber, M. Weckenbrock, A. Staudte, L. Spielberger, O. Jagutzki, V. Mergel, F. Afaneh, G. Urbasch, M. Vollmer, H. Giessen, and R. Dorner, Phys. Rev. Lett. **84**, 443 (2000).
[39] B. Feuerstein, R. Moshammer, D. Fischer, A. Dorn, C. D. Schroter, J. Deipenwisch, J. R. Crespo Lopez-Urrutia, C. Hohr, P. Neumayer, J. Ullrich, H. Rottke, C. Trump, M. Wittmann, G. Korn, and W. Sandner, Phys. Rev. Lett. **87**, 043003 (2001).
[40] N. Camus, B. Fischer, M. Kremer, V. Sharma, A. Rudenko, B. Bergues, M. Kubel, N. G. Johnson, M. F. Kling, T. Pfeifer, J. Ullrich, and R. Moshammer, Phys. Rev. Lett. **108** 073003 (2012).
[41] T. Nubbemeyer, K. Gorling, A. Saenz, U. Eichmann, and W. Sandner, Phys. Rev. Lett. **101** 233001 (2008).
[42] M. G. Littman, M. M. Kash, and D. Kleppner, Phys. Rev. Lett. **41**, 103 (1978).